

Trajectory statistics and turbulence evolution

M. Vlad and F. Spineanu

*National Institute of Laser, Plasma and Radiation Physics
Atomistilor 409, 077125 Magurele, Bucharest, Romania*

Abstract

The aim of this paper is to understand the tendency to organization of the turbulence in two-dimensional ideal fluids. We show that nonlinear processes as inverse cascade of the energy and vorticity concentration are essentially determined by trajectory trapping or eddying. The statistics of the trajectories of the vorticity elements is studied using a semianalytic method. The separation of the positive and negative vorticity is due to the attraction produced by a large scale vortex on the small scale vortices of the same sign. More precisely, a large scale velocity is shown to determine average transverse drifts, which have opposite orientations for positive and negative vorticity. They appear in the presence of trapping and lead to energy flow to large scales due to the increase of the circulation of the large vortex. Recent results on drift turbulence evolution in magnetically confined plasmas are discussed in order to underline the idea that there is a link between the inverse cascade and trajectory trapping. The physical mechanisms are different in fluids and plasmas due to the different types of nonlinearities of the two systems, but trajectory trapping has the main role in both cases.

Keywords: test particle statistics, turbulence, self-organization, vorticity, Euler fluid

1. Introduction

The two-dimensional fluid turbulence represented during more than 70 years an active field of research (see the review papers [1], [2], [3] and the references therein). It has many applications in different areas as fluid dynamics, meteorology, oceanography, fusion plasmas, superfluids, superconductors and astrophysics, in spite of the fact that it provides only idealized models for physical systems that are always three-dimensional.

The two-dimensional turbulence has a self-organizing character, which is related to the invariance of both energy and enstrophy in ideal (inviscid) fluids. Numerical studies of the decaying turbulence clearly show this property and the associated scaling behaviour [4], [5], [6]. The enstrophy has a direct cascade (to small scales), but with a complex evolution characterized by the presence of inverse cascade in isolated regions [7], [8]. The energy has an inverse cascade (to large scales) that leads to the emergence of large quasi coherent vortices. The process of self-organization can continue until the coherent vortices reach the size of the system [9], [10]. This behaviour was explained in the representation of point-like vortices by a negative temperature ([11], [1], [12]) or by the property of self-duality of the associated field theoretical model ([13]). The latter approach was extended to a model of planetary atmosphere and magnetized plasmas [14].

This paper deals with the turbulent states and studies the self-organization during its initial stage, before the emergence of large coherent vortices of the system size.

We show that trajectory trapping or eddying in the structure of the turbulence is the main physical reason for the strong nonlinear effects that are observed in two-dimensional ideal fluids. This conclusion is drawn from a study of the statistics of test particles (tracers) in turbulent Euler fluids.

This study is based on a series of recent results on the statistical properties of test particle trajectories in incompressible two-dimensional velocity fields. Numerical simulations have shown that trajectories are complex, as they have both random and quasi-coherent aspects. A typical trajectory, shown in Figure 1, is a random sequence of long jumps and trapping events that consists of winding on almost closed paths. Analytical methods that describe the statistics of these trajectories were developed [15], [16] and used for understanding various aspects of turbulent transport. It was shown that they provide a very good description of the nonlinear effects produced by trajectory trapping or eddying and reasonably accurate quantitative results for the diffusion coefficients and for other statistical averages.

The conclusion of these studies is that trajectory trapping or eddying leads to nonstandard statistics: memory effects (represented by long time Lagrangian correlation), strongly modified transport coefficients and non-Gaussian distributions of displacements. It was also shown that trapping determines a large degree of coherence in the sense that bundles of trajectories that start from neighboring points remain close for very long time compared to the eddying time. Trapped trajectories form quasi-coherent

structures similar to fluid vortices. Extensive theoretical [17]-[21] and numerical studies [22]-[24] have contributed significantly in the last decades to the understanding of the turbulent transport in laboratory or space plasmas, in fluids or in stochastic magnetic fields.

The connection between the test particle trapping and the turbulence evolution was discussed in [25] based on a study of test modes on turbulent plasmas. Analytical results that are in agreement with numerical simulations were obtained, and they allowed to deduce a new physical perspective on the nonlinear process of generation of large scale correlations (inverse cascade) and of zonal flow modes. Essentially, they are effects of ion trajectory trapping or eddying.

We show here that trapping has an essential role in two-dimensional fluid turbulence. A nonlinear effect produced by trapping of the vorticity elements explains the separation of positive and negative vorticity and the inverse cascade of the energy.

The paper is organized as follows. The problem of test particle or tracer transport is defined in Section 2.1 and Section 2.2 contains a short presentation of the analytical statistical approach, the decorrelation trajectory method (DTM). The effects of trapping or eddying on tracer transport and on the statistical characteristics of the trajectories are discussed in Section 3. This section contains a review of the previous work and new results on the modifications of the trajectory structures determined by an average velocity. The effects of trapping on the decaying two-dimensional turbulence in ideal fluids are analyzed in Section 4.1. The physical process that determines the separation of the positive and negative vorticity and leads to the inverse cascade of the energy is identified. The average speed of vorticity separation is estimated. Section 4.2 is a short discussion on recent results on plasma turbulence evolution, which show that trajectory trapping has an essential role in the inverse cascade, although the physical mechanism is completely different. The conclusions are summarized in Section 5.

2. Test particle transport and the statistical method

2.1. The problem

The problem of test particle or tracer advection in two-dimensional incompressible velocity fields is described by the stochastic equation:

$$\frac{d\mathbf{x}(t)}{dt} = \mathbf{v}[\mathbf{x}(t), t] + V_d \mathbf{e}_y, \quad (1)$$

where $\mathbf{x}(t)$ represents the trajectory in the plane ($\mathbf{e}_x, \mathbf{e}_y$) and $V_d \mathbf{e}_y$ is an average velocity that is taken in the \mathbf{e}_y direction. The stochastic velocity $\mathbf{v}(\mathbf{x}, t)$ is incompressible [$\nabla \cdot \mathbf{v}(\mathbf{x}, t) = 0$] and is represented by a scalar field, the stochastic potential or stream function

$$\mathbf{v}(\mathbf{x}, t) = \mathbf{e}_z \times \nabla \phi = (-\partial_y \phi, \partial_x \phi). \quad (2)$$

The potential $\phi(\mathbf{x}, t)$ is considered to be a stationary and homogeneous Gaussian stochastic field, with zero average and given two-point Eulerian correlation function (EC)

$$E(\mathbf{x}, t) \equiv \langle \phi(\mathbf{x}', t') v_j(\mathbf{x}' + \mathbf{x}, t' + t) \rangle \quad (3)$$

where $\langle \dots \rangle$ denotes the statistical average over the realizations of $\phi(\mathbf{x}, t)$ or the integral over \mathbf{x}' and t' . The main parameters of the EC are: the amplitude of the potential fluctuations $\beta^2 = E(\mathbf{0}, 0)$, the correlation length λ_c and the correlation time τ_c , which are the characteristic length and time of the decay of the function $E(\mathbf{x}, t)$. The EC's of the velocity components are obtained as space derivatives of $E(\mathbf{x}, t)$ and the amplitude of the stochastic velocity is $V = \beta/\lambda_c$.

Starting from the above statistical description of the stochastic potential and from an explicit EC one has to determine the statistical properties of the trajectories. This problem is nonlinear due to the space dependence of the potential, which leads to \mathbf{x} dependence of the EC (3).

The trajectories are solutions of a Hamiltonian system and thus, for time independent potential $\phi(\mathbf{x})$, their paths are the contour lines of the total potential $\phi(\mathbf{x}) + xV_d$ (the stream lines). The velocity is a continuous function of \mathbf{x} and t in each realization and it determines an unique trajectory as the solution Eq. (1) with the initial condition $\mathbf{x}(0) = \mathbf{0}$.

For $V_d = 0$ the stream lines are closed curves (with the exception of one contour line, $\phi(\mathbf{x}) = 0$, which extends to infinite), and the trajectories are periodic functions of time. They correspond to permanent trapping. This invariance property is approximately maintained for potentials that are weakly perturbed by a slow time variation. The trajectories approximately follow the contour lines of $\phi(\mathbf{x}, t)$ on almost closed paths for time intervals that are larger than the time of flight $\tau_{fl} = \lambda_c/V$. This leads to typical trajectories similar to the example shown in Figure 1. They have a complex structure that consists of a random sequence of trapping events and long jumps. Trapping appears at different scales when the particles are close

to the maxima or minima of the potential. The large displacements are produced when the trajectories are at small absolute values of the potential. The importance of trapping is measured by the Kubo number defined by

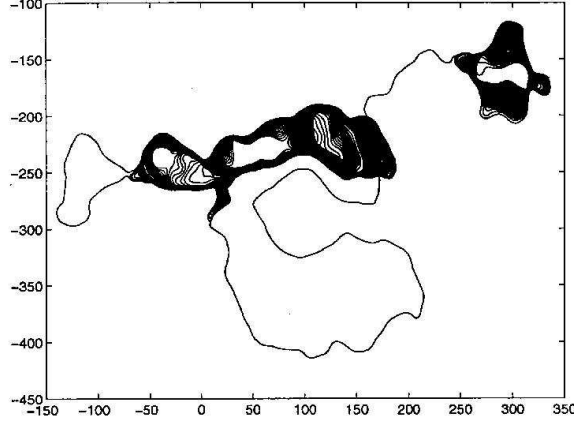


Figure 1: A typical trajectory obtained from Eq.(1) for $K = 10$, $V_d = 0$ and the stream function used in the simulations presented in [30].

$$K \equiv \frac{\tau_c}{\tau_{fl}} = \frac{V\tau_c}{\lambda_c}. \quad (4)$$

Trajectory trapping appears for $K > 1$ and becomes stronger as K increases up to the limit of static or frozen fields ($K, \tau_c = \infty$) when the trapping is permanent.

An average velocity V_d changes the topology of the total potential $\phi(\mathbf{x}) + xV_d$ by generating bunches of opened contour lines along its direction. When $r \equiv V_d/V < 1$, islands of closed contour lines persist between the bunches of opened lines, which enables trajectory trapping. At large average velocities $r \gg 1$ all the contour lines are opened and test particle cannot be trapped. The average velocity defines a characteristic time for traversing the correlation length with the average velocity, $\tau_* = \lambda_c/V_d$, and a dimensionless parameter similar to the Kubo number

$$K_* \equiv \frac{\tau_*}{\tau_{fl}} = \frac{V}{V_d} = \frac{1}{r}. \quad (5)$$

The condition that trapped trajectories are obtained from Eq. (1) is $K > 1$ and $K_* > 1$ (or $r < 1$).

Test particle transport is essentially determined by the Lagrangian velocity correlation (LVC) defined by

$$L_{ij}(t) \equiv \langle v_i [\mathbf{x}(0), 0] v_j [\mathbf{x}(t), t] \rangle \quad (6)$$

for a stationary process. As shown by Taylor [26], the mean square displacement $\langle x_i^2(t) \rangle$ and its derivative, the running diffusion coefficient $D_i(t)$, are integrals of the LVC

$$\langle x_i^2(t) \rangle = 2 \int_0^t d\tau L_{ii}(\tau) (t - \tau), \quad (7)$$

$$D_i(t) = \int_0^t d\tau L_{ii}(\tau). \quad (8)$$

The asymptotic values of $D_i(t)$

$$\chi_i = \lim_{t \rightarrow \infty} D_i(t) = \int_0^\infty L_{ii}(\tau) d\tau \quad (9)$$

are the diffusion coefficients. The time dependent diffusion coefficients provide the "microscopic" characteristics of the transport process. The diffusion at the transport space-time scales, which are much larger than λ_i and τ_c , is described by the asymptotic values χ_i .

The scaling of the diffusion coefficient in the Kubo number can be obtained by a simple estimation based on the general shape of the LVC (6). It is usually a function that decays to zero from the value V^2 at $t = 0$ in a characteristic time τ_d (the decorrelation time). For small Kubo numbers $K \ll 1$ ($\tau_c \ll \tau_{fl}$), the time variation of the velocity field is fast and the particles cannot "see" the space structure of the velocity field. In this quasilinear regime (or the weak turbulence case) $\tau_d = \tau_c$ and the diffusion coefficient (9) is $\chi_{ql} \approx V^2 \tau_c = (\lambda_c^2 / \tau_c) K^2$. In the nonlinear regime $K \gg 1$ ($\tau_{fl} \ll \tau_c$), the decay time of the LVC is $\tau_d = \tau_{fl}$ and the diffusion scales as the Bohm diffusion coefficient $\chi_B \approx V^2 \tau_{fl} = (\lambda_c^2 / \tau_c) K$, which does not depend on τ_c . The shape of the EC determines only a numerical factor in the diffusion coefficient.

The Bohm scaling does not apply in the case of diffusion in 2-dimensional divergence-free velocity fields described by Eq. (1). Numerical simulations have shown that the diffusion coefficient does not saturate as τ_c increases, but it decreases with the increase of the correlation time at $K > 1$ ($\tau_c > \tau_{fl}$).

Trajectory trapping or eddying was found to produce this effect [27]. The scaling in the nonlinear regime is

$$\chi_{tr} \approx (\lambda_c^2/\tau_c)K^\alpha = \beta K^{\alpha-1}, \quad (10)$$

where $\alpha < 1$. In particular, in the limit of static or frozen potential $K \rightarrow \infty$, the process is subdiffusive with $\chi_{tr} \rightarrow 0$.

2.2. The decorrelation trajectory method (DTM)

Several methods (as Corrsin approximation [28], [29], direct interaction approximation [30], the renormalization group technique [31]) were developed for determining the LVC corresponding to given EC. All these methods lead to finite diffusion coefficient of Bohm type in the limit $K \rightarrow \infty$, which shows that they are not adequate for the two-dimensional incompressible velocity fields. This process was studied especially by means of direct numerical simulations ([32] and the reference there in) or by developing simplified models [33]. There is a theoretical estimation [34] based on the analogy with the fractal structure of the landscapes. Using the theory of percolation, it finds the scaling of the diffusion coefficient of the type (10) with $\alpha = 0.7$. It is the first analytical estimation that has obtained subdiffusion in the frozen turbulence. The problem is that this method can provide only the scaling of χ , but not the statistics of the test particle trajectories.

Important analytical results in the study of this special case were obtained in the last decades by developing new statistical methods (the decorrelation trajectory method DTM [15] and the nested subensemble approach NSA [16]). They determine the LVC, the time dependent diffusion coefficients $D_i(t)$, the probability of displacements until decorrelation and other statistical averages. It was shown that the presence of trapping determines memory effects in $L(t)$ and a rich class of anomalous diffusion regimes in the presence of a decorrelation mechanism [16]. The trapping has also collective effects. It determines coherence in the stochastic motion in the sense that bundles of neighboring trajectories form localized structures similar to fluid vortices.

DTM reduces the problem of determining the statistical behavior of the stochastic trajectories to the calculation of weighted averages of smooth, deterministic trajectories obtained from the Eulerian correlation of the potential [15]. DTM is a semi-analytical statistical approach that satisfies the statistical consequences of the invariance of the potential.

The main idea of our approach is to study the stochastic equations (1) in subensembles of realizations of the stochastic field, which contain all realizations that have the same values of the stochastic potential and velocity in the starting point of the trajectories

$$(S) : \quad \phi(\mathbf{0}, 0) = \phi^0, \quad \mathbf{v}(\mathbf{0}, 0) = \mathbf{v}^0. \quad (11)$$

A average potential Φ^S and velocity \mathbf{V}^S exist in each subensemble. They are space-time dependent functions determined by the EC of the potential as

$$\Phi^S(\mathbf{x}, t) = \phi^0 \frac{E(\mathbf{x}, t)}{E(0, 0)} + v_x^0 \frac{E_y(\mathbf{x}, t)}{V_x^2} - v_y^0 \frac{E_x(\mathbf{x}, t)}{V_y^2}, \quad (12)$$

$$\mathbf{V}^S(\mathbf{x}, t) = \mathbf{e}_z \times \nabla \Phi^S(\mathbf{x}, t) \quad (13)$$

where $\mathbf{x} = (x, y)$, ϕ^0 , v_i^0 are the parameters of the subensemble and the subscripts represent derivatives ($E_i \equiv \partial E / \partial x_i$). The amplitudes of the velocities are $V_x^2 = -E_{yy}(\mathbf{0})$, $V_y^2 = -E_{xx}(\mathbf{0})$.

The stochastic equations are studied in each subensemble (S), where trajectories with a high degree of similarity are obtained due to the supplementary initial conditions (11). Neglecting the fluctuations of the trajectories, the average trajectory in (S) (*the decorrelation trajectory*) is obtained by averaging Eqs. (1) in (S). One obtains average equations with the same structure as the equations in each realization (1), but having the stochastic potential replaced by the subensemble (conditional) average potential

$$\frac{d\mathbf{X}^S}{dt} = \mathbf{e}_z \times \nabla \Phi^S + V_d \mathbf{e}_y. \quad (14)$$

This approximation is validated in [16], where it is shown that the DTM is the first order in a systematic expansion, and that the results obtained in the second order are close to those of the first order.

The Lagrangian correlations are obtained as averages over the decorrelation trajectories, by summing the contribution of each subensemble (S), weighted by the probability that a realization belongs to the subensemble. In particular, the LVC is approximated using the decorrelation trajectories as

$$L_{ii}(t) \cong \int d\phi^0 P(\phi^0) \int dv_1^0 dv_2^0 P(v_1^0) P(v_2^0) v_i^0 \frac{dX_i^S(t)}{dt}, \quad (15)$$

where P is the Gaussian probability

$$P(\phi^0) = \frac{1}{\sqrt{2\pi}\beta} \exp\left(-\frac{(\phi^0)^2}{2\beta^2}\right), \quad P(v_i^0) = \frac{1}{\sqrt{2\pi}V_i} \exp\left(-\frac{(v_i^0)^2}{2V_i^2}\right).$$

Thus, the DTM is essentially an analytical method, which determines the diffusion coefficients from a set of simple, deterministic trajectories that result from the EC of the stochastic field. However, in most cases, the DT's have to be numerically integrated. A computer code was developed for calculating the time dependent diffusion coefficients. It determines the DT's (14) for a large enough number of subensembles and performs the integrals in Eq.(15). These computer calculations are at PC level, for times of the order of 10 minutes.

3. Effects of trajectory trapping on test particle statistics

3.1. Memory effects and anomalous diffusion coefficients

The Lagrangian velocity correlation (LVC) determines the time dependent diffusion coefficient (8) and the mean square displacement (7). It is also a measure of the statistical memory of the stochastic motion.

The presence of trajectory trapping leads to a specific shape of the LVC for a frozen turbulence $\phi(\mathbf{x})$. This function decays to zero in a time of the order τ_{fl} but at later times it becomes negative, it reaches a minimum and then it decays to zero having a long, negative tail. The tail has a power law decay with an exponent that depends on the EC of the potential [35]. The positive and negative parts compensate such that the integral of $L(t)$, the running diffusion coefficient $D(t)$, decays to zero. The transport in such two-dimensional potential is thus subdiffusive. The tail of the LVC shows that the stochastic trajectories in frozen turbulence have long time memory. Thus, the LVC for incompressible two-dimensional velocity fields is completely different from the LVC of diffusion without trapping. The latter is decaying from V^2 to zero in a time of the order τ_{fl} .

This stochastic process is unstable in the sense that any weak perturbation produces a strong influence on the transport. A perturbation represents a decorrelation mechanism and its strength is characterized by a decorrelation time τ_d . The weak perturbations produce long decorrelation times, $\tau_d \gg \tau_{fl}$. In the absence of trapping, such a weak perturbation does not

produce a modification of the diffusion coefficient because the LVC is zero at $t > \tau_{fl}$. In the presence of trapping, which is characterized by long time LVC, such perturbation influences the tail of the LVC and destroys the equilibrium between the positive and the negative parts. Consequently, the diffusion coefficient is a decreasing function of τ_d . It means that when the decorrelation mechanism becomes weaker (τ_d increases) the transport decreases. This is a consequence of the fact that the long time LVC is negative. This behavior is completely different from that obtained in stochastic fields that do not produce trapping. In this case, the transport is stable to the weak perturbations, because the LVC is zero for $t > \tau_{fl}$. An influence of the decorrelation can appear only when the perturbation is strong such that $\tau_d < \tau_{fl}$ and it determines the increase of the diffusion coefficient with the increase of τ_d .

The decorrelation can be produced for instance by the time variation of the stochastic potential, which destroys the Lagrangian correlations at $t > \tau_c$. The transport becomes diffusive with an asymptotic diffusion coefficient that has the trapping scaling (10), and thus it is a decreasing function of τ_c . This behavior is determined by the fact that a stronger perturbation (with smaller τ_d) liberates a larger number of trapped trajectories, which contribute to the diffusion. For other types of perturbations, the interaction with the trapping process produces more complicated nonlinear effects. For instance, particle collisions lead to the generation of a positive bump on the tail of the LVC [19] due to the property of the 2-dimensional Brownian motion of returning in the already visited places.

The average velocity $V_d \mathbf{e}_y$ does not provide a decorrelation mechanism, but it determines an average potential that changes the structure of the contour lines by producing bunches of opened lines (as discussed in Section 2.1). A strong modification of the diffusion coefficient is produced by the average velocity in the presence of trajectory trapping ($K_* > 1$ and $K > 1$), which consists of a large increase of the parallel diffusion D_y and of the decrease of the perpendicular diffusion D_x [36]. Also, an interesting process of "acceleration" appears. Since a fraction of the trajectories n_{tr} are trapped, they cannot participate to the average flux, which is produced only by the free trajectories. The velocity field has zero divergence, thus the distribution of the Lagrangian velocity is time independent, and in particular, the average Lagrangian velocity is equal to V_d . Due to this, the average velocity of the free particles V_f has to be larger than V_d such that $n_f V_f = V_d$. Here $n_f = 1 - n_{tr}$ is the fraction of free trajectories. The increased velocity V_f is determined by the selection of the stochastic velocity along the opened contour lines of

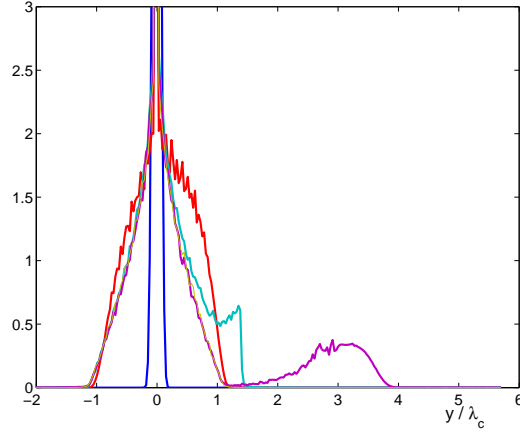


Figure 2: The probability of displacements along the average velocity $V_d \mathbf{e}_y$ obtained with the DTM for $K = 10$ and $r = V_d/V = 0.2$ at several time moments.

the potential, which are situated preferentially in regions where the Eulerian velocity is oriented along $V_d \mathbf{e}_y$. The trapping determines in these conditions a strong modification of the distribution of displacements, which elongates in the direction of $V_d \mathbf{e}_y$ and eventually it splits in two parts (see Figure 2).

The case of a stochastic potential that moves with the velocity $V_d \mathbf{e}_y$ is obtained by a Galilean transformation. This leads to opposite flows: trapped particles move with the potential and the free ones move in the opposite direction such that the total flux is zero, $n_{tr} V_d + n_f V_f = 0$.

3.2. Coherence and trajectory structures

The statistical characteristics of the trapped and of the free trajectories were studied in [16]. We have shown that the two types of trajectories have completely different statistical characteristics.

The trapped trajectories have a quasi-coherent behavior. Their average displacement, dispersion and probability of displacements saturate in a time τ_s . The time evolution of the square distance between two trajectories $\langle \delta x^2(t) \rangle$ is very slow showing that neighboring particles have a coherent motion for a long time, much longer than τ_s . They are characterized by a strong clump effect with the increase of $\langle \delta x^2(t) \rangle$ that is slower than the Richardson law. These trajectories form quasi-coherent structures which are similar to fluid vortices and represent eddying regions.

In time dependent potentials (with finite τ_c), the structures with $\tau_s > \tau_c$ are destroyed and the corresponding trajectories contribute to the diffusion

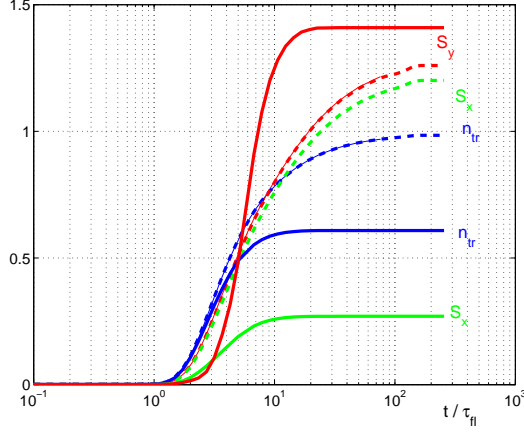


Figure 3: The formation of quasi-coherent trajectory structures in a time independent stream function ($K, \tau_c = \infty$). The time evolution of n_{tr} , S_x , S_y for $V_d = 0$ (dashed lines) and $V_d = 0.2$ (continuous lines).

process. These free trajectories have a continuously growing average displacement and dispersion. They have incoherent behavior and the clump effect is absent. The probability of short time displacements are non-Gaussian for both types of trajectories.

The study of vorticity separation (presented in Section 4.1) requires more information on the trajectory structures than obtained in [16]. It is necessary to determine the fraction of trapped trajectories n_{tr} and the average size of the structures S_i as functions of the average velocity V_d .

These statistical quantities are obtained using the DTM as weighted averages of the decorrelation trajectories $\mathbf{X}^S(t)$ in the static potential. The solutions of Eq. (14) are periodic functions in this case with the periods $T(\phi^0, \mathbf{v}^0)$ that depend on the subensemble. The fraction of trapped trajectories at time t is

$$n_{tr}(t) = \int d\phi^0 P(\phi^0) \int dv_1^0 dv_2^0 P(v_1^0) P(v_1^0) c_{tr}(t; \phi^0, \mathbf{v}^0), \quad (16)$$

where $c_{tr}(t; \phi^0, \mathbf{v}^0) = 1$ if $t > T(\phi^0, \mathbf{v}^0)$ and $c_{tr}(t; \phi^0, \mathbf{v}^0) = 0$ if $t < T(\phi^0, \mathbf{v}^0)$. The sizes of the trajectory structures on the $i = x, y$ directions are

$$S_i(t) = \int d\phi^0 P(\phi^0) \int dv_1^0 dv_2^0 P(v_1^0) P(v_1^0) X_i^{\max}(t; \phi^0, \mathbf{v}^0), \quad (17)$$

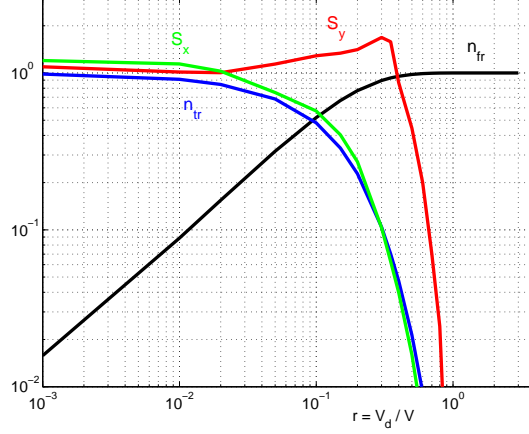


Figure 4: The dependence of the parameters of the quasi-coherent structures on the average velocity.

where $X_i^{\max}(t; \phi^0, \mathbf{v}^0) = \max(X_i^S)$ if $t > T(\phi^0, \mathbf{v}^0)$ and $X_i^{\max}(t; \phi^0, \mathbf{v}^0) = 0$ if $t < T(\phi^0, \mathbf{v}^0)$. These functions describe the growth of the trajectory structures.

The time evolution of the fraction of trapped trajectories $n_{tr}(t)$ and the average size of the structures $S_x(t)$, $S_y(t)$ are plotted in Figure 3 for $V_d = 0$ (dashed lines) and for $V_d = 0.2$ (continuous lines). For $V_d = 0$, the structures continuously grow due to the large size stream lines that lead to large periods of the corresponding trajectories. An average velocity generates bunches of opened lines of the total potential and limits the size of the islands of closed contour lines. The size of the structures and $n_{tr}(t)$ saturate at finite V_d , as seen in Figure 3. The average velocity determines the decrease of n_{tr} and of the size of the structures in the perpendicular direction S_x , while the parallel size S_y is increased. The structures are elongated by the velocity.

The saturation values of the parameters of the structures n_{tr} , S_x , S_y and $n_f = 1 - n_{tr}$ are plotted in Figure 4 as functions of V_d . One can see that the trajectory structures exists only for small average velocities with $r = V_d/V < 1$ (or $K_* > 1$). When $r \gtrsim 1$, the structures are destroyed by the average velocity, which opens all the contour lines of the total potential.

4. Effects of trapping on turbulence evolution

The idea of the strong relation between tracer trapping or eddying and turbulence evolution is sustained by analyzing two completely different phys-

ical systems: the relaxation of turbulence in two-dimensional ideal fluids and the drift turbulence in magnetically confined plasmas. Fluids are stable and turbulence is externally produced by steering, while inhomogeneous plasmas are unstable and generate spontaneously turbulence. However, both systems are characterized by the inverse cascade of the energy in the evolution of turbulence and by the tendency to self-organization. We show that in both cases these processes are determined by trajectory trapping, but with different mechanisms, which are essentially determined by the different nonlinearities of the systems. The case of fluid turbulence is analyzed in Section 4.1, where the statistics of the trajectories of the vorticity elements in the neighborhood of a large vortex is studied. Section 4.2 contains a short review of recent results on the evolution of the drift turbulence in magnetically confined plasmas. It is introduced in order to underline the idea that trajectory trapping has the main role in both cases, despite the fact that the physical processes that determine the inverse cascade are completely different.

4.1. *Ideal fluids*

Ideal fluids are described by the Euler equation

$$\partial_t \omega + \mathbf{v} \cdot \nabla \omega = 0, \quad (18)$$

$$\mathbf{v} = \mathbf{e}_z \times \nabla \phi, \quad (19)$$

$$\omega = \Delta \phi, \quad (20)$$

where ω is the vorticity, ϕ is the stream function and \mathbf{v} is the fluid velocity. Thus vorticity elements are advected by the velocity field and the vorticity is conserved on the trajectories. The nonlinearity of the process is determined by the relations (19)-(20) between \mathbf{v} and ω , which show that vorticity is an active field.

Numerical simulations have shown that the vorticity field evolves to organized states characterized by isolated vorticity peaks with large amplitudes. A process of separation of positive and negative vorticity and vorticity concentration occurs during the relaxation of turbulent states. Our aim is to understand how is possible to appear vorticity separation in a turbulent state.

In order to study this tendency, we consider a turbulent state as initial condition of Eq. (18) that is represented by a stochastic stream function

with Gaussian distribution and with the Eulerian correlation $E(\mathbf{x})$. We have taken for the results presented in the figures

$$E(\mathbf{x}) = E(r) = \frac{2 - 5r^2 + r^4}{2} \exp\left(-\frac{r^2}{2}\right), \quad (21)$$

where $r = |\mathbf{x}|/\lambda$. This function is normalized to $E(\mathbf{0}) = 1$ and its space integral is zero. The latter condition is due to the choice of the total vorticity equal to zero. The presence of a large scale vortex is modeled by an average stream function $\langle\phi(\mathbf{x})\rangle = xV_d$ that accounts for an average velocity $V_d\mathbf{e}_y$. We consider first an uniform velocity, and the effect of a small transverse gradient of $V_d\mathbf{e}_y$ is discussed at the end of this section.

Trajectory trapping occurs when $K_* > 1$ and $K > 1$, as discussed in Section 3.1. The first condition implies large amplitudes of the stochastic component of the velocity compared to the average velocity $V > V_d$. The second condition corresponds to large correlation times of the stochastic stream function $\tau_c > \tau_{fl} = \lambda_c/V$. The temporal evolution of the stream function is determined in ideal fluids by the motion of the vorticity elements, which modifies the vorticity field. This process is slow compared to the time of flight, which means that fluid turbulence has $K > 1$. Thus, trapping occurs in two-dimensional fluid turbulence when the average velocity is zero or small ($V_d < V$).

The stream function and the vorticity are correlated and their two-point correlation function results from $E(\mathbf{x})$ using Eq. (20)

$$E_{\phi\omega}(\mathbf{x}) \equiv \langle\phi(\mathbf{x}') \omega(\mathbf{x}' + \mathbf{x})\rangle = \triangle E(\mathbf{x}) \quad (22)$$

Thus, the stream function and the vorticity in the same point ($\mathbf{x} = \mathbf{0}$) have opposite signs since $E(\mathbf{0})$ is the maximum of $E(\mathbf{x})$ and $\triangle E(\mathbf{0}) < 0$. This correlation, determined by the nonlinearity of the fluid flow, has an important role in vorticity separation.

The trajectories of the vorticity elements are solutions of Eq. (1). Since they are independent on the vorticity and on its sign, it is not evident how vorticity separation can occur.

We show that the average velocity $V_d\mathbf{e}_y$ determines two transverse flows with opposite directions. They appear in the presence of eddying and their direction is correlated with the sign of the stream function corresponding to the stream line on which the trajectory is trapped.

The average displacement of the vorticity elements is determined using DTM by summing the contributions of all subensembles. An equation similar to (15) is obtained

$$\langle \mathbf{x}(t) \rangle = \int d\phi^0 P(\phi^0) \int d\mathbf{v}^0 P(\mathbf{v}^0) \mathbf{X}^S(t), \quad (23)$$

where $\mathbf{X}^S(t)$ is the decorrelation trajectory in the subensemble S determined from Eq. (14). The component perpendicular on the average velocity is zero. Actually it is of the order 10^{-5} , which is the accuracy of the numerical calculation. This is the correct result for an incompressible velocity field. The average Lagrangian velocity has to be equal to the Eulerian average velocity, which has no component in the \mathbf{e}_x direction. However, the conditional average displacement for a given value of the initial stream function ϕ^0

$$\langle x(t) \rangle_{\phi^0} = P(\phi^0) \int d\mathbf{v}^0 P(\mathbf{v}^0) X^S(t) \quad (24)$$

is not zero, but it is an anti-symmetrical function of ϕ^0 , as shown in Figure 5. One can see that the displacements are correlated with the stream function and that $\langle x(t) \rangle_{\phi^0}$ and of ϕ^0 have the same sign. The displacements are negligible at small time when there is no trapping. As time increases, the maximum of $|\langle x(t) \rangle_{\phi^0}|$ increases and eventually saturates.

Due to the anti-correlation of the stream function and vorticity in the same point ($E_{\phi\omega}(\mathbf{0}) < 0$), the positive peaks of the stream function correspond to negative vorticity, while the negative ones correspond to positive vorticity. Thus the correlation of the perpendicular displacement with the stream function corresponds to a correlation between displacements and vorticity.

The total average displacements for positive ϕ^0 , $\langle x(t) \rangle_+$, and respectively for negative ϕ^0 , $\langle x(t) \rangle_-$, are represented in Figure 6. They are symmetrical and compensate, as required by the zero divergence of the velocity field. These average displacements determine opposite average velocities in the case of time dependent vorticity fields

$$V_{s+} = \frac{\langle x(\tau_c) \rangle_+}{\tau_c}, \quad V_{s-} = \frac{\langle x(\tau_c) \rangle_-}{\tau_c} = -V_{s+}, \quad (25)$$

where τ_c is the correlation time.

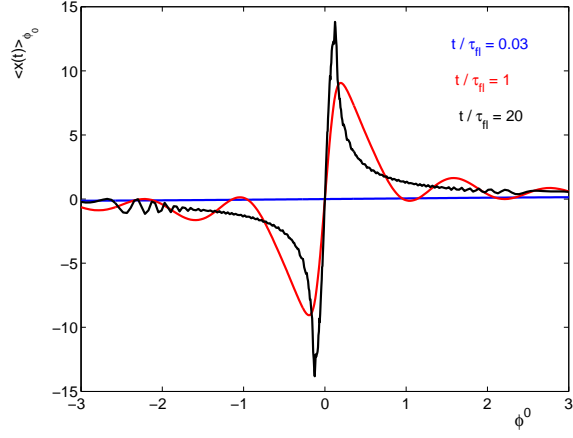


Figure 5: The average perpendicular displacement as function on the initial stream function for $r = V_d/V = 0.2$ and $K = \infty$.

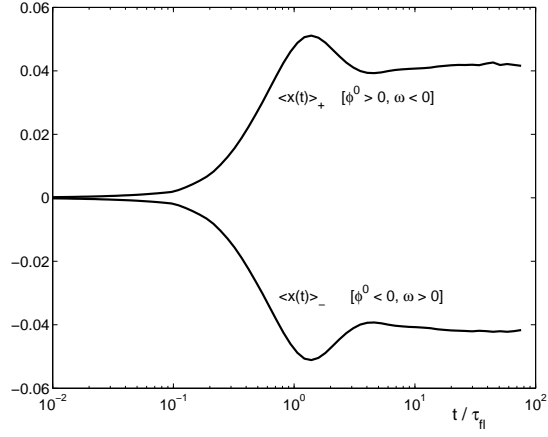


Figure 6: The average perpendicular displacements for the positive and negative vorticity ($r = V_d/V = 0.2$ and $K = \infty$).

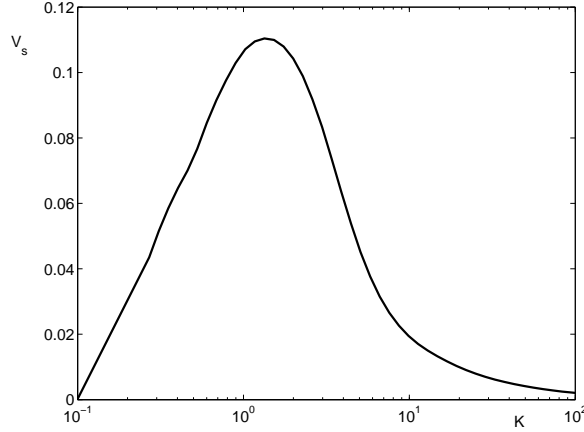


Figure 7: The average normalized velocity of positive and negative vorticity separation, V_s/V as function of the Kubo number for $r = 0.2$.

In terms of vorticity, the negative vorticity elements that are trapped on the stream lines with $\phi^0 > 0$ move with the velocity V_{s+} in the direction of the gradient of the large scale stream function. The positive vorticity elements have an opposite average velocity. Thus, the positive and negative vorticity elements that evolve on trapped trajectories separate with a speed $V_s = V_{s+} - V_{s-} = 2V_{s+}$. This speed is plotted in Figure 7 as function of the Kubo number $K = \tau_c/\tau_{fl}$. One can see that V_s is maximum for K of the order one, and it decays at $K \gg 1$ as K^{-1} due to the saturation of the average displacements. The maximum value is smaller than V_d , but not negligible.

The physical mechanism for the vorticity separation consists of the influence of the average velocity on the small structures of trapped trajectories. V_d determines a difference between the average velocities on the two sides of the closed trajectories that are oriented along $V_d \mathbf{e}_y$. The velocity is $\partial_x \phi + V_d$ on one side and $\partial_x \phi - V_d$ on the other side. The difference of velocities leads to the accumulation of the vorticity elements on the small velocity side and to the increase of the vorticity in that region. As the direction of the velocity on the contours of ϕ depend on the sign of ϕ , the accumulation of the vorticity elements occurs on opposite sides for contours corresponding to ϕ and $-\phi$. The time variation of the velocity field destroys the trajectory structures in a time of the order τ_c , and the coherent displacements of the vorticity elements produce transverse average velocities.

The average displacement $\langle y(t) \rangle$ along the average velocity $V_d \mathbf{e}_y$ is produced, as explained in Section 3.1, only by the free trajectories. They determine the elongation and eventually the splitting of the distribution of displacements (see Figure 2). Thus, the vorticity elements spread along $V_d \mathbf{e}_y$ while they have transverse drifts.

The average flows of the vorticity elements determine the modification of the vorticity distribution. Due to the correlation (22), this changes the distribution of the stream function: the contour lines of the stream function follow the average motion of the vorticity.

These findings are in agreement with the image provided by the numerical simulations (see for instance [37]), which show the emergence of large vortices that elongate and attract small vortices of the same sign. We note that the process analyzed here is different from the vortex drift transverse to a sheared flow analyzed in [38] since it involves vorticity elements in turbulent flows and not localized vortices. In our case the drift is produced by an average velocity and the existence of a gradient of the background vorticity is not necessary.

A vortex determines a velocity that has a gradient in the transverse direction. The gradient length is much larger than the correlation length of the stream function in the case of a large vortex in a small scale stochastic velocity field. In these conditions, the effects of the gradient can be estimated using the dependence on V_d of the statistical characteristics obtained at constant V_d .

The transverse drift of the small structures with the same sign of the vorticity as the large vortex is in the direction of the gradient and brings the structure toward larger V_d . This determines the decrease of the transverse dimension of the structure and the increase of its elongation, as seen in Figure 4. When $V_d \gtrsim V$, the small structures are destroyed. The fraction of trapped trajectories and the size of the structures decrease rapidly for $V_d > V$. Their vorticity is included in the large vortex, and it leads to the increase of the large scale energy (inverse cascade). On the contrary, the structures with opposite sign of vorticity drift toward smaller V_d , against the gradient. Their size increases and their elongation is reduced.

In conclusion, a large size vortex in a decaying two-dimensional turbulence attracts the small size vortices with the same sign of vorticity while the small vortices of the opposite sign are repelled. This effect of vorticity separation according to its sign is produced by trapping of the vorticity elements combined with the existence of the correlation of the stream function with

the vorticity imposed by the nonlinearity (20).

4.2. Drift turbulence

The nonlinear stage in the evolution of drift type turbulence is essentially a consequence of ion trajectory trapping or eddying in the structure of the stochastic potential. This conclusion is drawn from a study of test modes on turbulent plasmas [25], [39] based on a new Lagrangian approach that extends the type of methods initiated by Dupree [40] to the nonlinear regime characterized by trapping. Drift waves are unstable due to the electron kinetic effects that produce the dissipation mechanism to release the energy, combined with the ion polarization drift [41]. Beside this, the polarization drift has a more complex influence determined by its nonzero divergence, which produces a weak compressibility effect in the background turbulence.

Test modes on turbulent plasmas were studied for drift turbulence in constant magnetic field starting from the basic description provided by the drift kinetic equations. Analytical expressions are derived, which approximate the growth rate $\gamma(\mathbf{k})$ and the frequency $\omega(\mathbf{k})$ of a test mode with wave number $\mathbf{k} = (k_x, k_y)$ as functions of the characteristics of the background turbulence. These functions provide the tendency of turbulence evolution.

The dispersion relation of the test modes in turbulent plasma is shown to be the same as in quiescent plasma, except for a time dependent function $M(t)$, which embeds all the effects of the background turbulence. This function appears in the propagator of the test mode, which is obtained using the formal solution of the ion equation with the method of characteristics. The characteristics are ion trajectories in the stochastic background potential. They are described by equations similar to Eq. (1), with the difference that the potential ϕ is moving with the effective diamagnetic velocity $V_d \mathbf{e}_y$, which leads to the replacement of y with $y' = y - V_d t$. The function $M(t)$ is evaluated using the DTM, and the dispersion relation is analytically solved.

Drift turbulence develops in the initial stage on a wide range of wave numbers. Ion trajectories are not trapped at these small amplitudes of the background turbulence and they have Gaussian distribution. Their diffusion determines the damping of the large wave number modes. The correlation lengths λ_i remain close to the ion Larmor radius ρ_i during this stage. Turbulence amplitude β increases and the shape of the EC is not changed.

When the amplitude reaches values that make $K_* > 1$, ion trajectory trapping appears and generates vortical structures of trapped ions as discussed in Section 3.2. They determine the decrease of the frequencies, which

leads to the decrease of γ and to the displacement of the unstable range of wave numbers to smaller values. The maximum of the growing rate is displaced from $k_y \cong 1/\rho_i$ to $k_y \cong 1/S$, where S is the average size of trajectory structures. Turbulence amplitude continues to increase in this stage, but with a smaller rate. This determines the increase of the fraction of the trapped ions n_{tr} and of the size S of the trajectory structures.

Large scale correlations are generated through a nonlinear process of decreasing the wave number of the unstable modes. In the same time, the diffusive damping produced by the free trajectories continues to act on the large \mathbf{k} modes, which are attenuated. This process of inverse cascade of turbulence energy stops well before the size of the potential cell becomes comparable with the system size. A different effect appears at larger trapping rates, which is also connected with trapping.

When the fraction of trapped ions n_{tr} becomes comparable with the fraction of free ions n_f , ion flows are generated by the trapping process as explained in Section 3.1. Trapped ions move with the potential, while free ions move in the opposite direction such that the total flux is zero. This determines the splitting of the distribution of ion displacement (as in Figure 2). As shown in [25], an essential change of test modes is produced. The drift modes are damped and a different type of modes, zonal flow modes, are generated in this strongly nonlinear regime. They have $k_y = 0$ and very small frequencies and are produced by the combined action of the ion flows and of the compressibility due to the polarization drift in the background turbulence. The damping of the drift modes is not determined by the zonal flow modes as generally believed. There is only an indirect contribution through the diffusive damping, which is increased by the zonal flow modes [39]. The decay of the drift turbulence determines the decrease of n_{tr} and of the growth rate of the zonal flow modes, which is proportional to n_{tr} . Consequently, drift turbulence does not saturate, but it oscillates between weak and strong trapping. The predator-prey paradigm is not sustained by these results, although there is time correlation between the growth of zonal flow modes and the damping of the drift modes.

In conclusion, trapping determines in the first phase the increase of the correlation length by displacing the range of unstable modes to small $k \sim 1/S$. In the second stage, when it becomes stronger and produces ion flows in the moving background turbulence, trapping leads to the nonlinear damping of the drift modes. In the same time, trapping combined with the polarization drift generates zonal flow modes.

5. Conclusion

Particle motion in two-dimensional incompressible stochastic velocity fields is characterized by a mixture of random and quasi-coherent aspects, represented by a random sequence of large jumps and trapping or eddying events. Trajectory trapping generates quasi-coherent structures of trajectories.

The development of statistical methods that are adequate for the description of such complex trajectories has contributed to the understanding of the nonstandard characteristics of the transport in these systems. Various aspects of the turbulent transport were analyzed in the test particle approach using these semi analytical methods. These studies are now in a new stage that consists of developing Lagrangian methods for the study of the evolution of the turbulence in the nonlinear regime. First results are reported in [25] and in the present paper. They lead to the conclusion that trajectory trapping has the essential role in turbulence evolution. The physical mechanism depends on the specific nonlinearity of each system, but it is related to trajectory trapping. It appears that the quasi-coherent component of the trajectories determine the nonlinear effects in turbulence while the random component provides a damping or dissipation process.

In the case of fluids, the trapped vorticity elements have an average motion, which leads to average velocities with the directions dependent on the vorticity sign. Then, due to the correlation $E_{\phi\omega}$, the stream function is also transported by the perpendicular average flows. The effect of this process is the separation of the vorticity with different signs since negative vorticity moves in the sense of the stream function gradient and positive vorticity in the opposite sense. A small gradient of the average velocity that characterizes a large scale vortex determines the decrease of the attracted small vortices and eventually the inclusion of their vorticity in the large vortex. This process determines the flow of the energy from small to large scales.

In the case of drift turbulence, the trapped ions determine the displacement of the wave numbers of the most unstable modes towards small values, while the free ions contribute to the diffusive damping of the large k modes. The correlation length of the stochastic potential increases until the process of nonlinear damping becomes dominant. Ion trapping has an important role in this process and also in the generation of the zonal flow modes.

Acknowledgments This work was supported by the Romanian Ministry of National Education under the contract PN 09 39 01 01.

References

- [1] Kraichnan R H, Montgomery D. Rep. Progr. Phys. 1980;43:547-619.
- [2] Provenzale A. Annu. Rev. Fluid Mech. 1999;31:55–93.
- [3] Kukharkin N N. J. Scientific Computing 1995;10:409-448.
- [4] McWilliams J. J. Fluid Mech. 1984;146:21-43.
- [5] Weisse J, McWilliams J. Phys. Fluids A 1993; 5:608-621.
- [6] Maassen S R, Clercx H J H, van Heijst G J F. Phys. Fluids 2002;14:2150-2169.
- [7] Ohkitani K. Phys. Fluids A 1991;3:1598-1611.
- [8] Babiano A, Provenzale A. J. Fluid Mech. 2007;574:429-448.
- [9] Matthaeus W H, Stribling W T, Martinez D, Oughton S, Montgomery D. Phys. Rev. Lett. 1991; 66:2731–2735.
- [10] Montgomery D, Matthaeus W H, Stribling W T, Martinez D, Oughton S. Phys. Fluids A 1992; 4:3–6.
- [11] Edwards S F, Taylor J B. Proc. R. Soc. Lond. A 1974;336:257–271.
- [12] Robert R, Sommeria J. Phys. Rev. Lett. 1992;69:2776–2779.
- [13] Spineanu F, Vlad M. Phys. Rev. E 2003;67:046309.
- [14] Spineanu F, Vlad M. Phys. Rev. Lett. 2005;94:235003.
- [15] Vlad M, Spineanu F, Misguich J H, Balescu R. Phys. Rev. E 1998;58:7359-7368.
- [16] Vlad M, Spineanu F. Phys. Rev. E 2004;70:056304.
- [17] Vlad M, Spineanu F, Misguich J H, Balescu R. Phys. Rev. E 2003;67:026406.
- [18] Vlad M, Spineanu F. Astrophys. J. 2014; 791:56.

- [19] Vlad M, Spineanu F, Misguich J H and Balescu R 2000 Phys. Rev. E 61 3023.
- [20] Petrisor I, Negrea M, Weyssow B. Physica Scripta 2007; 75:1-12.
- [21] Neur M, Spatschek K H. Phys.Rev. E 2006;74:036401.
- [22] Zimbardo G, Veltri P, Pommois P. Phys. Rev. E 2000;61:1940-1948.
- [23] Hauff T, Jenko F, Shalchi A, Schlickeiser R. Astrophysical J. 2010;711:997-1007.
- [24] Beresnyak A, Yan H, Lazarian A. Astrophys. J. 2011; 728:60.
- [25] Vlad M. Phys. Rev. E 2013;87:053105.
- [26] Taylor G I. Proc. London Math. Soc. 1921; 20:196.
- [27] Kraichnan R H. Phys. Fluids 1970;13:22-31.
- [28] Corrsin S. Advances in Geophysics 6. Atmospheric Diffusion and Air Pollution, 161. New York:Academic;1959.
- [29] McComb W D. The Physics of Fluid Turbulence, Oxford: Clarendon; 1990.
- [30] Roberts P H, J. Fluid Mech. 1961;11:257.
- [31] Bouchaud J P, George A. Phys. Reports 1990;195:127-293.
- [32] Reuss J D, Vlad M, Misguich J H. Phys. Lett. A 1998;241:94-98.
- [33] Majda A J, Kramer P R. Phys. Reports 1999; 314:237-574.
- [34] Isichenko M B. Rev. Mod. Phys. 1992;64:961-1043.
- [35] Vlad M, Spineanu F, Misguich J H, Reuss J D, Balescu R, Itoh K, Itoh S I. Plasma Phys. Control. Fusion 2004; 46:1051-1063.
- [36] Vlad M, Spineanu F, Misguich J H and Balescu R 2001 Phys. Rev. E 63 066304.
- [37] McWilliams J. J. Fluid Mech. 1990;219:361-385.

- [38] Schecter D, Dubin D. Phys Fluids 2001;13:1704-1723.
- [39] Vlad M, Spineanu F. Phys. Plasmas 2013;20:122304.
- [40] Dupree T H. Phys. Fluids 1966;9:1773-1782.
- [41] Goldstone R J, Rutherford P H. *Introduction to Plasma Physics*, Institute of Physics Publishing, Bristol and Philadelphia, 1995.